

Diversity in peptide recognition by the SH2 domain of SH2B1

Marissa A. McKercher¹ | Xiaoyang Guan² | Zhongping Tan² | Deborah S. Wuttke¹ 

¹Department of Chemistry and Biochemistry, University of Colorado, Boulder, Colorado

²Department of Chemistry and Biochemistry, BioFrontiers Institute, University of Colorado, Boulder, Colorado

Correspondence

Deborah S. Wuttke, Department of Chemistry and Biochemistry, UCB 596, University of Colorado, Boulder, Colorado 80309, USA.

Email: deborah.wuttke@colorado.edu

Funding information

The National Science Foundation, Directorate for Biological Sciences, MCB1121842; Division of Chemistry, CHE1454925

Abstract

SH2B1 is a multidomain protein that serves as a key adaptor to regulate numerous cellular events, such as insulin, leptin, and growth hormone signaling pathways. Many of these protein-protein interactions are mediated by the SH2 domain of SH2B1, which recognizes ligands containing a phosphorylated tyrosine (pY), including peptides derived from janus kinase 2, insulin receptor, and insulin receptor substrate-1 and -2. Specificity for the SH2 domain of SH2B1 is conferred in these ligands either by a hydrophobic or an acidic side chain at the +3 position C-terminal to the pY. This specificity for chemically disparate species suggests that SH2B1 relies on distinct thermodynamic or structural mechanisms to bind to peptides. Using binding and structural strategies, we have identified unique thermodynamic signatures for each peptide binding mode, and several SH2B1 residues, including K575 and R578, that play distinct roles in peptide binding. The high-resolution structure of the SH2 domain of SH2B1 further reveals conformationally plastic protein loops that may contribute to the ability of the protein to recognize dissimilar ligands. Together, numerous hydrophobic and electrostatic interactions, in addition to backbone conformational flexibility, permit the recognition of diverse peptides by SH2B1. An understanding of this expanded peptide recognition will allow for the identification of novel physiologically relevant SH2B1/peptide interactions, which can contribute to the design of obesity and diabetes pharmaceuticals to target the ligand-binding interface of SH2B1 with high specificity.

KEY WORDS

affinity, crystallography, multimodal specificity, NMR, SH2 domain, signaling

1 | INTRODUCTION

SH2B1 is a key adaptor protein, found in several species including humans and mice,¹ that activates numerous cellular pathways in response to external stimuli including insulin, leptin, and growth hormone exposure.^{2–5} As a result, SH2B1 is a key regulator of glucose metabolism and body weight, with possible roles in the management of obesity and diabetes.^{2,6} Upon binding of hormone molecules to transmembrane receptors, SH2B1 is recruited from the cytosol to the membrane where it can either interact directly with the receptor (e.g., insulin receptor (IR)^{7–10}) or with other receptor-localized cytosolic proteins, such as janus kinase 2 (JAK2)^{11–16} or insulin receptor substrate-1 and -2 (IRS1 and IRS2).^{3,6} The interaction between SH2B1 and JAK2 has been especially well studied, and this interaction is known to increase the catalytic activity of JAK2 *in vivo*, resulting in enhanced auto-phosphorylation or phosphorylation of substrate molecules.^{14,17,18} Many of the interactions between SH2B1 and ligands, including JAK2, are mediated by the SRC Homology 2 (SH2) domain of SH2B1, which

binds phosphotyrosine (pY)-containing ligands upon auto- or transphosphorylation of the ligand. Through numerous additional structural elements, including a pleckstrin homology (PH) domain, dimerization domain (DD), proline-rich sequences, and posttranslational modifications (including several phosphorylated tyrosines), SH2B1 can bind multiple targets simultaneously. This role as an adaptor allows SH2B1 to spatially bridge regulatory proteins to form large signaling complexes capable of eliciting diverse cellular activities.

Several high-throughput array studies, which probed binding of SH2 domains to libraries of degenerate peptide sequences¹⁹ or of approximately 6200 phosphopeptides derived from the human proteome,²⁰ found the SH2 domain of SH2B1 to have a preference for peptides with predominantly hydrophobic amino acids at the positions immediately C-terminal to the pY. An especially strong specificity for a leucine or isoleucine at the +3 position (the third amino acid C-terminal to the pY) was identified.²⁰ The preference for a small hydrophobic amino acid at the +3 position is supported by the interaction between the SH2 domain of SH2B1 and a peptide derived from JAK2

(JAK2-pep), which contains a +3 leucine. The structure of SH2B1/JAK2-pep reveals a narrow uncharged peptide-binding surface (Supplemental Figure 1), which provides a clear rationale for the observed preference for peptide ligands containing hydrophobic residues at the +3 position.²¹ The +3 Leu forms hydrophobic contacts to four nearby ($<4.0\text{ \AA}$) residues (V589, L592, I609, and L611) and more distal hydrophobic contacts (between 4.0 and 5.0 \AA) to three additional residues (L577, F604, and P610). Together, these seven residues form a narrow hydrophobic binding groove between the EF and BG loops of SH2B1, thereby creating a favorable pocket for binding to hydrophobic peptide ligands.

Interestingly, several studies using smaller libraries of <200 physiological peptides derived from specific signaling systems (e.g., ErbB or insulin signaling proteins) identified an unexpected preference of SH2B1 for peptides with aspartic acid (Asp) or glutamic acid (Glu) at the +3 position.^{22,23} For example, a study using 192 phosphopeptides derived from proteins involved in fibroblast growth factor (FGF), insulin growth factor (IGF-1), and insulin signaling pathways found that, while capable of binding hydrophobic peptides, the SH2 domain of SH2B1 also bound preferentially to acidic peptides.^{22,23} The specificity profile was identified as pY-X-X-(D/E/φ), where X represents any of the 20 standard amino acids, and φ represents hydrophobic amino acids.²³ Similarly, a study using a library of 92 phosphopeptides corresponding to ErbB receptor intracellular tyrosine sites found seven sites capable of binding to SH2B1 with affinities tighter than $20\text{ }\mu\text{M}$, as determined by high-throughput fluorescence polarization (HT-FP).²⁴ All seven peptides contained one or more Asp or Glu residues within the three positions (+1, +2, +3) C-terminal to the pY, and three peptides contained an Asp or Glu residue specifically at the +3 position. It is unclear how SH2B1 accommodates these acidic peptides based on the hydrophobic pocket apparent in the existing structure of the primary binding conformation of SH2B1 bound to JAK2-pep,²¹ suggesting that SH2B1 has additional binding modes that allow it to bind acidic peptides from diverse physiological origins.

The use of multiple binding modes may be a mechanism shared amongst numerous SH2 domains, as we have previously observed similar multimodal peptide binding specificity in the C-terminal SH2 domain (PLCC) of phospholipase C-γ1. Similar to the chemically diverse ligands observed to bind SH2B1, peptide array studies have demonstrated that PLCC also binds peptides containing amino acids of dissimilar size and polarity.^{19,20,22,23,25,26} We previously showed that PLCC contains a chemically diverse interface, including a charged residue (R716) and numerous hydrophobic residues, that predominantly drives the recognition of an expanded repertoire of binding partners. An overlay of several peptide-bound structures of the SH2 domain of SRC reveals similar behavior to PLCC, in which several polar or hydrophobic residues in the EF and BG loops promote the accommodation of numerous conformationally distinct ligands (PDB IDs: 1SHA, 1SHB, 1P13, 1NZL, 1HCS, and 1SPS). The SH2 domain of interleukin-2 tyrosine kinase (Itk), also utilizes multiple binding modes to accommodate diverse ligands. This is accomplished through *cis-trans* isomerization of a single proline residue (Pro287) within Itk, which promotes a reorientation of

the CD loop that modulates conformer-specific recognition of exclusive subsets of ligands.^{27,28}

We have explored how SH2B1 exhibits specificity for peptides from two distinct chemical classes using structural and thermodynamic approaches. We have identified several flexible SH2B1 loops and specific amino acids that distinctly impact binding to peptides containing hydrophobic versus acidic residues at the +3 position. We have further demonstrated electrostatic interactions to residues K575 and R578 to be key for peptide recognition. Multimodal specificity may allow SH2B1 to participate in previously unrecognized signaling pathways through interactions with an expanded set of pY targets. This knowledge increases our understanding of the role of SH2B1 as a signaling hub in metabolic pathways, and may aid in determining the pathways by which SH2B1 regulates body weight and glucose metabolism in humans.^{2,6} Consequently, the identification of diverse modes of peptide recognition by SH2B1 may have significant implications for the rational design of therapeutics targeting the SH2B1/ligand interface for the treatment of obesity and diabetes.

2 | MATERIALS AND METHODS

2.1 | SH2B1 cloning, expression, and purification

A pGEX6P1 plasmid containing DNA for residues 515–639 of human SH2B1 was a gift from Bruce Mayer (Addgene plasmid #46479).²⁹ SH2B1 (residues 519–628) was amplified out of pGEX6P1 and subcloned into pET15b using BamH1 and Nde1 restriction enzymes. Desired mutations (e.g., K575E and R578E) to SH2B1 were made by site-directed mutagenesis (QuikChange method, Agilent Technologies). SH2B1 was expressed in BL21 (DE3) *E. coli*, lysed by sonication in lysis buffer (100 mM potassium phosphate, pH 7.2, 200 mM NaCl, 1 mM DTT, and 25 mM imidazole), purified by nickel affinity and size-exclusion chromatography, and cleaved from the 6X-His tag by thrombin protease as previously described for the C-terminal SH2 domain of phospholipase C-γ1.³⁰ Analysis by SDS-PAGE indicated $>98\%$ purity. Typical protein yields were approximately 40 mg/L. For isotopically labeled protein, SH2B1 was grown in minimal media with $(^{15}\text{NH}_4)_2\text{SO}_4$, as well as ^{13}C -glucose when intended for carbon-labeled experiments,³¹ and otherwise expressed and purified as described above.

2.2 | Synthesis of peptides

The desired phosphorylated peptides were synthesized on an Applied Biosystems Pioneer continuous flow peptide synthesizer under standard automated Fmoc conditions, as previously described.³⁰ Following purification by high-performance liquid chromatography (HPLC), peptide products were assessed for composition and purity by positive electrospray ionization mass spectrometry (ESI+ MS).

2.3 | Protein and peptide concentrations

Concentrations of SH2B1 were measured by absorbance at 280 nm, using the extinction coefficient calculated using ProtParam ($15470\text{ M}^{-1}\text{ cm}^{-1}$ for wildtype protein, and 9970 for SH2B1_3Δ).³²

TABLE 1 Sequences of the SH2B1-binding phosphopeptides^a

Peptide name	Protein of origin	Phosphorylated tyrosine	Sequence
JAK2-pep	Janus kinase 2	Y148	FTP D -pY- ELLTEN
ErbB4-pep	Receptor tyrosine kinase ErbB4	Y1202	AEDE -pY- VNEPLY
IR-pep	Insulin receptor	Y1158	TRDI -pY- ETDYYR
AN32A-pep	Acidic nuclear phosphoprotein 32 family member A	Y148	YLDG -pY- DRDDKE
IGF1R-pep	Insulin-like growth factor 1 receptor	Y1280	EVSF -pY- YSEENK

^aThe canonical peptide (JAK2-pep) contains a small, aliphatic, hydrophobic amino acid (Leu) at the +3 position. Four additional peptides, which contain acidic Asp (D) or Glu (E) residues at the +3 position (bold), are also capable of binding SH2B1.^{22–24} All peptide sequences were derived from human signaling proteins. The locations of tyrosine phosphorylation within the full-length proteins of origin are also indicated.

Concentrations of peptides were measured by absorbance at 205 nm using extinction coefficients calculated by manually summing the absorbance at 205 nm of the constituent amino acids (43792 M⁻¹ cm⁻¹ for JAK2-pep, 41301 M⁻¹ cm⁻¹ for ErbB4-pep, 49461 M⁻¹ cm⁻¹ for IR-pep, 42261 M⁻¹ cm⁻¹ for AN32A-pep, and 49770 M⁻¹ cm⁻¹ for IGF1R-pep).^{33,34}

2.4 | Isothermal titration calorimetry (ITC)

SH2B1 was dialyzed overnight at 4°C into buffer containing 25 mM Tris, pH 7.2, and 100 mM NaCl. The post-dialysis buffer was used to resuspend the peptides to ensure that the protein and peptide buffers were as closely matched as possible. Binding reactions were performed using a MicroCal iTC200 calorimeter at 35°C as previously described.³⁵ The temperature was raised from the standard 25°C in order to increase the observed heat release upon protein/peptide binding, as many of the interactions exhibited little enthalpic change at 25°C. Briefly, the sample cell was loaded with 203 μL of peptide at a concentration ranging from 20 to 100 μM. SH2B1 at an 8- to 10-fold higher concentration was titrated in as follows: one 0.2 μL dummy injection, 19 2 μL injections, and a final 1.3 μL injection, summing to a total of 39.5 μL of peptide used. Titration of SH2B1 into peptide (rather than peptide into SH2B1) significantly reduced background heats that likely resulted from the dilution of trace amounts of trifluoroacetic acid (TFA) that carried over from peptide synthesis and purification. Data were integrated and fit by nonlinear least-squares fitting to a single binding site model using Origin ITC Software (OriginLab, Northampton, MA). Prior to fitting, background heat from mixing or dilution effects were accounted for by subtracting the enthalpy observed in control experiments (titrating buffer into peptide and SH2B1 into buffer). All experiments were at a minimum repeated in triplicate.

2.5 | Crystallization

Protein/peptide solution was made by mixing 12 mg/mL SH2B1_3Δ (SH2B1 containing E583A, E584A, and W593H mutations) with a 1.4-fold molar excess of peptide ErbB4-pep in crystal buffer (50 mM potassium phosphate, pH 7.2, and 100 mM NaCl) at 4°C. The crystallization drop contained 0.5 μL of protein/peptide solution and 0.5 μL of mother liquor (30% PEG 3350, 200 mM K₂SO₄, and 40 mM phenol). Crystals

were grown by sitting drop vapor diffusion in 96-well trays set up using a Crystal Phoenix drop setter robot (Art Robbins Instruments). Crystals were cryoprotected by sequential transfer into solutions of mother liquor with an additional 5%, 10%, and 15% (v/v) glycerol.

2.6 | X-ray data collection and refinement

X-ray diffraction data was collected at the Advanced Light Source beamline 8.2.2. Reflections were indexed using MOSFLM,³⁶ and scaled using Scala³⁷ within the CCP4 program suite.³⁸ For a preliminary data set (for a crystal which diffracted to 1.7 Å resolution), molecular replacement using the Phaser program³⁹ within CCP4 was achieved using the coordinates of a free state of SH2B1 (PDB ID: 2HDV) as the starting model.²¹ For the final data set (for a crystal that diffracted to 1.4 Å resolution), our previous 1.7 Å data set was used for molecular replacement. A phosphate ion and three phenol molecules were manually built into the model based on clear electron density using Coot.⁴⁰ The model underwent multiple rounds of refinement using PHENIX Refine⁴¹ as well as manual adjustments made in Coot. The final model was evaluated using MolProbity to assess quality.⁴² Statistics are listed in Supplemental Table 1.

2.7 | Nuclear magnetic resonance (NMR) spectroscopy binding affinity analysis

NMR spectra for binding affinity analyses were collected at the W. M. Keck High Field 800 MHz NMR Facility on an Oxford 800 MHz magnet equipped with an Agilent console and HCN PFG room temperature probe. We utilized settings loaded with Biopack pulse sequences (gNhsqc.c for ¹H-¹⁵N-heteronuclear single-quantum coherence (¹H-¹⁵N-HSQC) experiments) available with the VnmrJ software, with minor modifications. Data were processed with NMRPipe⁴³ and visualized with CcpNmr Analysis.⁴⁴

¹H-¹⁵N-HSQC experiments for the determination of binding affinity were collected at 25°C on 20 μM of ¹H-¹⁵N-labeled SH2B1 in NMR buffer (50 mM Tris, pH 7.4, 50 mM NaCl, 1 mM Na₂EDTA, 1 mM DTT) with 10% D₂O and 150 μM TSP. A concentration of 20 μM SH2B1 was used for binding experiments because this was the lowest the concentration could be dropped ([Protein] ≪ K_d is a necessary assumption for this binding model) while maintaining sufficient signal to noise to

detect the chemical shifts. Unlabeled phosphopeptide at a concentration of 800 μ M was titrated into SH2B1, and 12 additional ^1H - ^{15}N -HSQC experiments were collected at the following molar ratios of peptide: 0.1, 0.25, 0.4, 0.55, 0.75, 1, 1.25, 1.50, 2, 3, 5, and 8. For weak binding peptide/protein interactions, an additional experiment using 12-fold molar excess of peptide was also collected. The K_d of the SH2B1/peptide interactions were determined by plotting the observed chemical shift ($\Delta\delta_{\text{obs}}$) versus total peptide ligand ($[\text{L}]_0$) at each titration point, and fitting the following equation using the Solver add-in available in Microsoft Excel.⁴⁵

$$\Delta\delta_{\text{obs}} = \Delta\delta_{\text{max}} \frac{(K_d + [\text{L}]_0 + [\text{P}]_0) - \sqrt{(K_d + [\text{L}]_0 + [\text{P}]_0)^2 - (4[\text{P}]_0[\text{L}]_0)}}{2[\text{P}]_0}$$

2.8 | NMR chemical shift mapping

All NMR spectra used for chemical shift mapping experiments and backbone assignments were collected at 25°C on an Oxford 600 MHz magnet equipped with an Agilent console and HCN PFG cold probe. Backbone resonance assignments for SH2B1 were obtained from HNCA, HN(CO)CA, HNCACB, and CBCA(CO)NH spectra, which were performed at 25°C on 1 mM ^1H - ^{15}N - ^{13}C -labeled SH2B1 in NMR buffer. These three-dimensional experiments were also performed on SH2B1/JAK2-pep, since this system was in the slow-exchange regime and, thus, backbone assignments could not be confidently transferred from the spectrum of the free protein. All other peptide systems were in the intermediate- to fast-exchange regime, allowing for the straightforward transfer of assignments from the free to peptide-bound states of SH2B1 without the need for additional carbon-labeled experiments.

^1H - ^{15}N -HSQC experiments used for chemical shift mapping were collected on 250 μ M of ^1H - ^{15}N -labeled SH2B1 in NMR buffer as previously described.³¹ A high protein concentration (250 μ M SH2B1) was used in order to achieve sufficient signal to noise to collect data in a short time (approximately 80 min per titration point). Unlabeled phosphopeptide was resuspended in NMR buffer to a concentration of 4–12 mM and titrated into SH2B1 in 0.25 molar ratio increments to a final protein to peptide ratio of 1:1.5. The observed chemical shift change ($\Delta\delta_{\text{obs}}$) for each amino acid upon peptide addition was calculated using the following equation:⁴⁶

$$\Delta\delta_{\text{obs}} = \sqrt{(\Delta\delta_{\text{H}})^2 + (0.17 \times \Delta\delta_{\text{N}})^2}$$

All chemical shift perturbations were visualized on the structure of SH2B1_3 Δ (PDB: 5W3R) using PyMOL.⁴⁷ Each amino acid of SH2B1 was colored in accordance with its classification as having a negligible, small, medium, or large chemical shift perturbation upon peptide binding using the following ranges: $\Delta\delta < 0.07$ ppm (negligible, green), $0.07 < \Delta\delta < 0.10$ ppm (small, yellow), $0.10 < \Delta\delta < 0.15$ ppm (medium, orange), and $\Delta\delta > 0.15$ ppm (large, red). Amino acids that did not produce any observed chemical shift (prolines or residues that are exchange broadened at these conditions) are colored in grey. Specifically, in addition to prolines, the following residues of free SH2B1 did not produce an observable chemical shift: M518, G530, G544, T546, Q571, E612, S613, S616, and S617.

3 | RESULTS

3.1 | SH2B1 binds acidic peptides with physiologically relevant affinities

Several array studies have demonstrated that the SH2 domain of SH2B1 has specificity for peptides containing small hydrophobic residues, especially leucine, at the +3 position C-terminal to the phosphotyrosine,^{19,20} which drives SH2B1 binding to canonical peptides derived from signaling proteins such as JAK2-pep. Although JAK2-pep contains several acidic residues (+1 Glu and +5 Glu), the structure of SH2B1/JAK2-pep demonstrates that peptide specificity is predominantly achieved through a network of hydrophobic contacts to the +3 leucine.²¹ Surprisingly, however, numerous peptides derived from insulin and ErbB receptor signaling pathways have also been shown to bind SH2B1, even though they contain acidic amino acids at the +3 position.^{22–24} To investigate the specificity of SH2B1 for +3 acidic residue-containing peptides, four of these putative binding peptides (ErbB4-pep, IR-pep, AN32A-pep, and IGF1R-pep) were chosen for additional binding and structural characterization (Table 1).

ITC and NMR ^1H - ^{15}N -HSQC titration experiments were used to study the affinities of SH2B1-binding phosphopeptides (Figure 1). Three of the peptides (ErbB4-pep, IR-pep, and AN32A-pep) bind SH2B1 with affinities in the range reliably quantifiable by both methods, which served to cross-validate these two equilibrium techniques. The affinities measured by both techniques were highly similar (within a 1.6-fold difference) which supports the direct comparison of affinities measured by ITC and NMR (Supplemental Table 2).

All five peptides bind SH2B1, with affinities ranging from 320 nM to 68 μ M (Table 2). The canonical peptide JAK2-pep binds the tightest, with an affinity of 320 ± 21 nM, which is within 2-fold of a previously measured affinity for this interaction at slightly different conditions (550 ± 10 nM).²¹ Notably, ErbB4-pep (which contains a +3 Glu) binds SH2B1 with an affinity of 542 ± 87 nM, which is only a 1.7-fold lower affinity than JAK2-pep (which has a hydrophobic +3 Leu). ErbB4-pep and JAK2-pep are consequently classified as tight affinity binders to SH2B1. These affinities are well within the range typical for physiologically relevant SH2 domain/ligand interactions,⁴⁸ suggesting that ErbB4-pep may have physiological implications in SH2B1 signaling pathways *in vivo*. However, although ErbB4-pep binds SH2B1 with similar affinity as cognate JAK2-pep, the thermodynamics underlying the interactions are very distinct. Cognate JAK2-pep binding to SH2B1 is entropically unfavorable and, consequently, is entirely driven by strong enthalpic contributions. In contrast, the ErbB4-pep interaction is driven by favorable entropies with only mild enthalpic contributions.

The three remaining peptides (IR-pep, AN32A-pep, and IGF1R-pep), which all contain an acidic Asp or Glu at the +3 position, also bind SH2B1 but demonstrate approximately 50- to 200-fold weaker affinities than JAK2-pep and ErbB4-pep (Table 2). They have consequently been classified as weak affinity binders. The three weak binders had similar thermodynamic signatures as ErbB4-pep, with strong entropic and mild enthalpic contributions, suggesting these are characteristic of the acidic peptide binding mode. Although these peptides

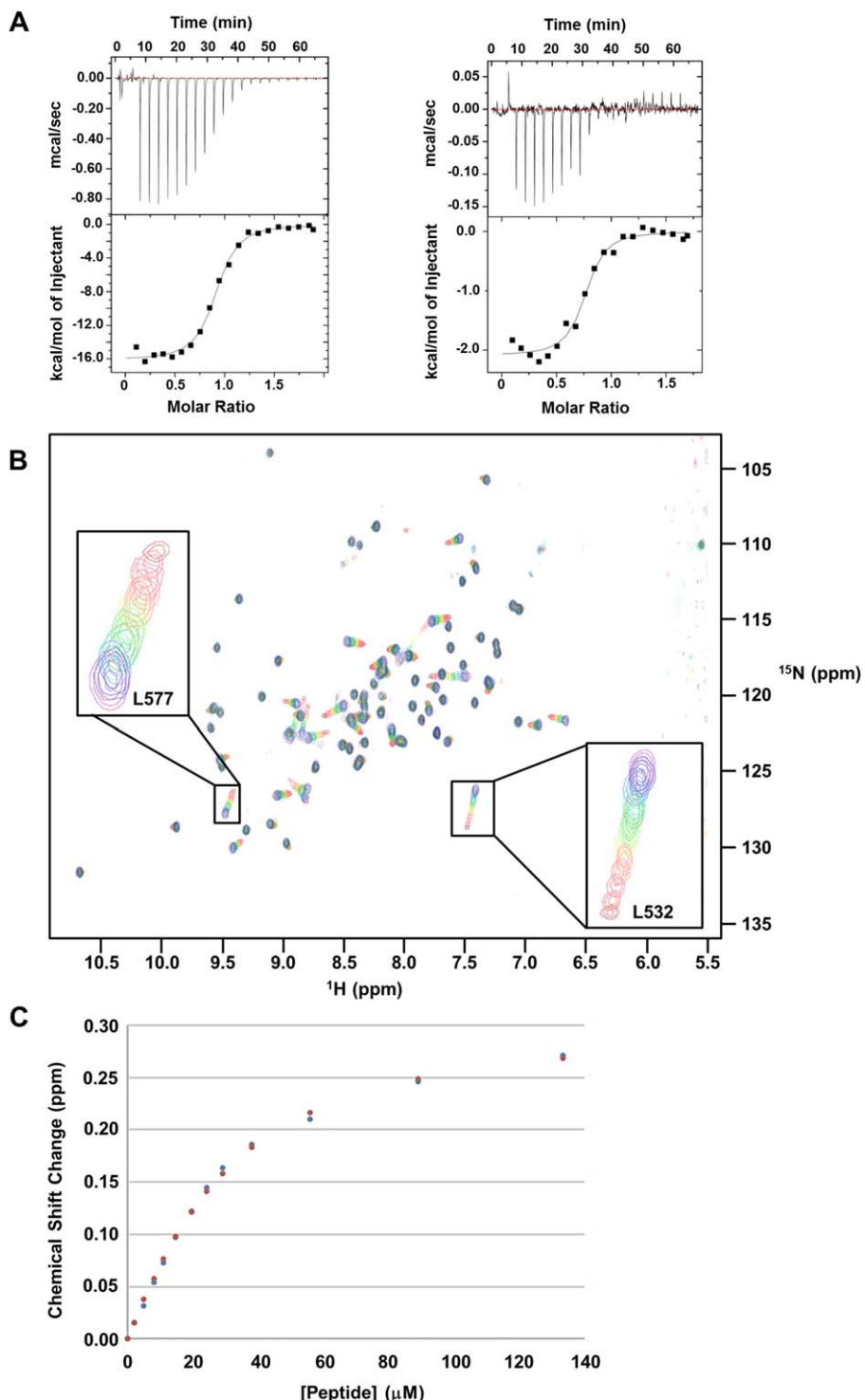


FIGURE 1 Representative ITC and NMR data for SH2B1/peptide interactions. A, ITC binding data for the titration of SH2B1 into JAK2-pep (left) and ErbB4-pep (right). The top panels are the raw heat signals upon protein titration, while the bottom panels show the integrated heat signals. SH2B1 binds JAK2-pep with an affinity of 320 ± 21 nM, while the K_d for ErbB4-pep is 542 ± 87 nM. Figure was created using Origin ITC Software (OriginLab, Northampton, MA). B, ^1H - ^{15}N -HSQC NMR titration experiments were used for binding affinity determination for the weaker micromolar peptides. The data shown are the titration of increasing concentrations of non-cognate peptide IR-pep into 20 μM ^1H - ^{15}N -labeled SH2B1. Free SH2B1 is shown in purple, while spectra of SH2B1 in the presence of increasing concentrations of IR-pep are shown in rainbow color order up to 160 μM (8-fold molar excess peptide), in dark red. The insets highlight residues L532 and L577, which illustrate peak "walking" behavior characteristic of a fast-exchange system. Data were visualized with the CcpNmr Analysis software.⁴⁴ C, Binding curve comparing the chemical shift changes of residue L577 as a function of the concentration of IR-pep added to SH2B1. The binding curve compares the observed chemical shift changes (blue) versus values calculated for a perfect 30.3 μM interaction (red). Values were calculated using the Solver add-in available in Microsoft Excel⁴⁵.

TABLE 2 Summary of SH2B1/phosphopeptide binding affinities^a

Peptide	Residue at +3 position	Affinity class	K _d (μM)	K _d Fold Change from JAK2-pep	ΔH by ITC (kcal/mol)	TΔS by ITC (kcal/mol)
JAK2-pep	L	Tight	0.320 ± 0.021 *	1	-16.1 ± 0.1	-6.89 ± 0.11
ErbB4-pep	E		0.542 ± 0.087 *	1.7	-2.17 ± 0.08	6.70 ± 0.18
IR-pep	D	Weak	30.3 ± 0.3	95	-1.20 ± 0.06	5.57 ± 0.19
AN32A-pep	D		18.2 ± 0.1	57	-1.70 ± 0.10	5.15 ± 0.13
IGF1R-pep	E		68.2 ± 2.6	210	n/a	n/a

^aThe tight affinity class interactions were assessed by ITC (indicated by an asterisk*), while weaker interactions were measured by NMR titration experiments. For the four peptide systems that could be studied by ITC, the enthalpy and entropy are also reported. Values shown are averages from a minimum of triplicate measurements. Error values reported are the standard errors of the mean.

share the acidic residue at position +3, ErbB4-pep binds to SH2B1 with a substantially tighter affinity, suggesting that our original bimodal peptide classification (hydrophobic versus acidic) was overly simplistic and that, rather, ErbB4 represents a third class of peptide ligand distinct from the other three acidic peptides.

3.2 | Crystal structure of free SH2B1 identifies several conformationally flexible loops

To structurally characterize the cognate and non-cognate peptide binding modes of SH2B1, crystals were grown of a triple-mutated version of SH2B1 (SH2B1_3Δ) when in the presence of a molar excess of each peptide. The SH2B1_3Δ construct, containing E583A, E584A, and W593H mutations, was used for crystallization based on previous findings that these mutations improved the ability of SH2B1 to crystallize with no impact on peptide binding affinity.²¹ In agreement with what has been previously shown, we also found that the triple mutation had little impact on peptide binding affinity. SH2B1_3Δ binds to peptides JAK2-pep and IR-pep with binding affinities of 195 ± 23 nM and 40.9 ± 8.0 μM, as measured by triplicate ITC experiments, which is within approximately 2-fold of the affinities measured by ITC of these peptides for wildtype SH2B1 (320 ± 21 nM and 18.8 ± 4.8 μM, respectively, Supplemental Table 2).

Following rigorous screening and crystal seeding approaches, high quality crystals of free SH2B1_3Δ were obtained. Although crystals of peptide-bound SH2B1_3Δ remained elusive, a comparison of multiple crystal structures in different packing geometries of free SH2B1 can establish the degree of inherent flexibility of the protein. The crystal belongs to spacegroup P2₁2₁2₁, with a single molecule of SH2B1_3Δ comprising the asymmetric unit. The structure of free SH2B1_3Δ was refined to a resolution of 1.4 Å (Figure 2A, PDB ID: 5W3R) with an R factor for the working set of reflections of 0.144 and a free R factor of 0.168 for the final model.

The structure is generally similar to the previously solved high-resolution crystal structure of SH2B1_3Δ (PDB ID: 2HDV), with root mean square deviation (RMSD) values of under 2.0 Å for all atoms when compared to both molecular chains of the previously published structure. Significant differences, however, are apparent in the DE loop, with RMSD values of approximately 4.9 Å (calculated for all

atoms of residues 580–587) and backbone movements up to nearly 9 Å (Figure 2B). A careful review of the structure, however, indicates that the DE loop conformation may be influenced by crystal packing contacts (Supplemental Figure 2). Nevertheless, it had sufficient flexibility to adopt a highly distinct structure.

Interpretable electron density for the BG loop (residues 611–618) was also obtained from the SH2B1_3Δ crystal, which highlights additional conformational flexibility. In the existing published 2.0 Å resolution structure of SH2B1_3Δ (PDB ID: 2HDV), electron density was lacking for the residues of the BG loop, which resulted in their omission from the final model. In the 1.4 Å structure presented here, the residues of loop BG were fit into clear electron density, allowing for the complete structure of the free protein to be modeled (Figure 2B). We note, however, that the conformation of the BG loop may be influenced by contacts between several BG loop residues (specifically 612E and 613S) and a neighboring symmetry mate molecule (Supplemental Figure 2). Furthermore, high temperature factors (B factors) for residues in the BG loop suggest that this loop remains relatively disordered, and may be conformationally flexible. While the average temperature factor for the entire SH2 domain is 15.7, the average for the BG loop is much higher (approximately 33.3). This agrees with ¹H-¹⁵N-HSQC NMR data (discussed below), where we demonstrate that chemical shift data is lacking for most of the BG loop residues in free SH2B1, suggesting the residues sample multiple different chemical environments. Taken together, the BG loop conformation presented here is likely stabilized by lattice contacts, whereas when in solution, the loop may adopt multiple conformations.

The EF and BG loops also take on substantially different conformations when compared to the complete structure of the SH2B1_3Δ/JAK2-pep complex (PDB ID: 2HDX, 1.5 Å resolution) (Figure 2C, D). The EF loop (residues 588–592) differences do not appear to be artifacts of crystal packing (Supplemental Figure 2). In the presence of JAK2-pep, the EF and BG loops undergo significant conformational rearrangements, with atomic movements up to 10 Å, which are likely necessary to sterically permit peptide binding (Figure 2D). These movements may also allow for the formation of numerous hydrophobic contacts known to form between JAK2-pep and residues I609, P610, and L611 of the BG loop (Supplemental Figure 1). With the ability to undergo conformational movements of nearly 10 Å, the BG loop may

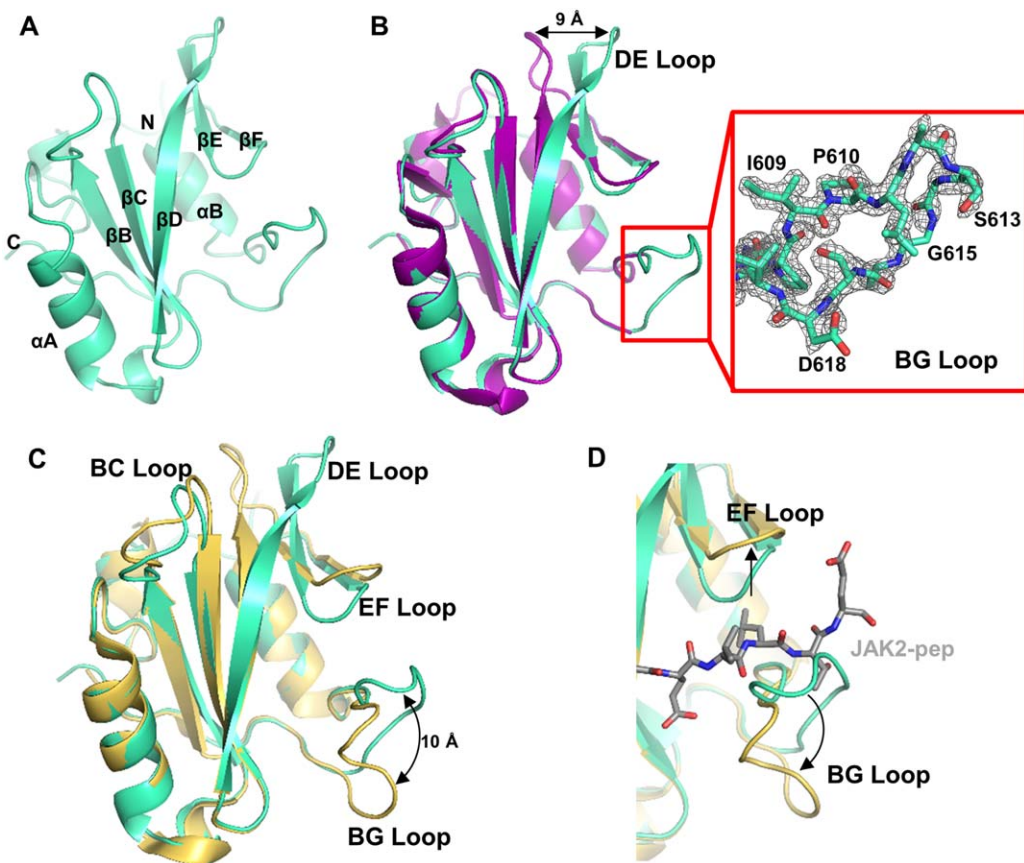


FIGURE 2 Comparison of free SH2B1_3Δ structures and the structure of the SH2B1_3Δ/JAK2-pep complex. A, Crystal structure of free SH2B1_3Δ, refined at a resolution of 1.4 Å (PDB ID: 5W3R, green). Secondary structure elements are labeled in accordance with nomenclature established by Eck et al. (1993).⁵⁶ B, When compared to the previously solved crystal structure of SH2B1_3Δ (PDB ID: 2HDV, chain A, purple), the backbone remains largely static, with the exception of the DE loop, which shifts by approximately 9 Å. The structure of the BG loop, which could not be built into the previous model due to a lack of electron density, was also determined. The inset shows the electron density for the BG loop residues, contoured to 1.0 σ . C, An overlay of free SH2B1_3Δ (green) compared to the previously solved crystal structure of the SH2B1_3Δ/JAK2-pep complex (PDB ID: 2HDX, chain A, yellow, JAK2-pep omitted for clarity). Minor conformational changes were observed in the DE, BC, and EF loops, and a significant shift of up to 10 Å was observed in the BG loop. D, When the JAK2-pep structure is included (grey), it is apparent that the outward movements of the EF and BG loops are likely necessary to sterically permit JAK2-pep binding. Images were created with PyMOL.⁴⁷

be able to adjust its conformation to also interact tightly with peptides that contain an acidic amino acid at the +3 position, such as ErbB4-pep. These findings suggest that the BG, DE, and EF loops exhibit inherent conformational flexibility, capable of moving several angstroms to accommodate ligand binding, which may contribute to the ability of SH2B1 to recognize diverse ligands.

3.3 | NMR chemical shift mapping data suggest SH2B1 uses a similar binding interface to bind diverse peptides, but also reveals several protein interactions unique to tight-binding peptides

The crystal structures of free SH2B1 and SH2B1/JAK2-pep highlight several regions of backbone flexibility that may facilitate the ability of the protein to bind canonical JAK2-pep and acidic residue-containing ErbB4-pep with comparable affinities. To explore possible differences in the ligand-binding interface of SH2B1 when bound to these two

tight affinity peptides, and to contrast this with the three weak binding peptides, NMR chemical shift mapping titration experiments were employed. ^1H - ^{15}N -HSQC NMR spectra were collected of SH2B1 as a function of added unlabeled peptide, and the chemical shift of each crosspeak monitored. Amide proton/nitrogen pairs that experienced significant chemical shift perturbations were mapped onto the surface of SH2B1 to compare and contrast the likely binding modes of the peptides. This approach can identify the most likely peptide-binding interface of SH2B1, as well as detect regions of the protein that undergo significant structural rearrangements upon peptide binding.

These data reveal that the two tight binding peptides, JAK2-pep and ErbB4-pep, likely share a conserved binding interface. This is indicated by numerous significant chemical shift perturbations observed for amino acids in the β D-strand of the central β -sheet, near the canonical pY binding pocket (Figure 3 and Supplemental Figure 3). Chemical shift perturbations were also observed for positively charged K575 and R578 residues (Supplemental Table 3), which allude to

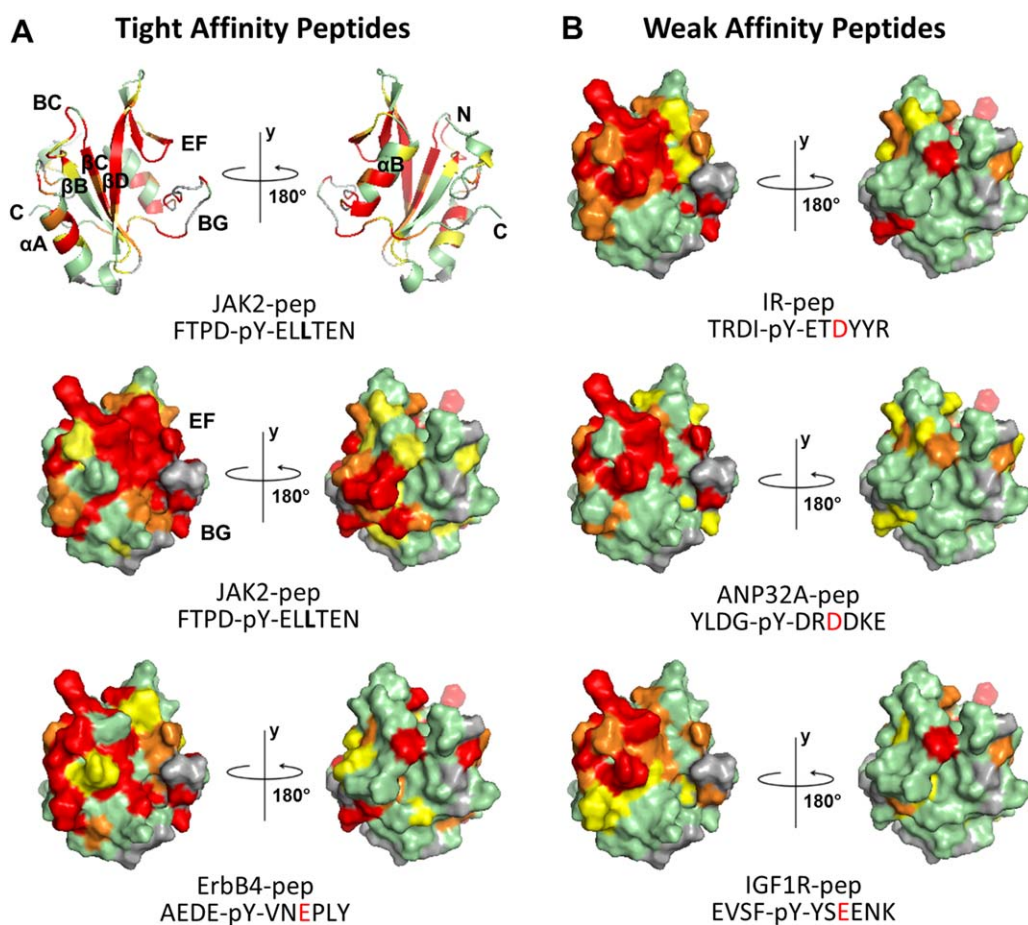


FIGURE 3 Chemical shift mapping of ^1H - ^{15}N -HSQC NMR peptide titration data highlights several differences between tight and weak peptide binding modes to SH2B1. Chemical shift perturbations were mapped onto the ribbon or surface representation of SH2B1_3 Δ (PDB ID: 5W3R) and colored as follows: $\Delta\delta < 0.07$ ppm (green), $0.07 < \Delta\delta < 0.10$ ppm (yellow), $0.10 < \Delta\delta < 0.15$ ppm (orange), $\Delta\delta > 0.15$ ppm (red), and unobserved chemical shifts (grey). Loop EF is labeled on the structure of SH2B1 to highlight the loop in which the most distinct differences can be observed between each peptide binding mode. Loop BG is also indicated. Chemical shift data is lacking for many of the residues in loop BG (colored grey), which may indicate conformational heterogeneity. A, Chemical shift mapping upon titration of tight binding peptides JAK2-pep, which contains a leucine at the +3 position (bold), and ErbB4-pep, which contains a glutamic acid at the +3 position (bold red). B, Chemical shift mapping upon titration of three weak binding peptides that contain negatively charged residues at the +3 position (bold red). Images were created with PyMOL⁴⁷.

electrostatic contributions to the peptide binding events. Hydrophobic amino acids known to contact the +3 Leu of JAK2-pep, including V589 and I609, are also significantly impacted by the addition of both JAK2-pep and ErbB4-pep, suggesting that ErbB4-pep maintains hydrophobic contacts to SH2B1 even in the absence of a hydrophobic residue at the +3 position.

However, several differences between the tight affinity peptides were also observed, which may indicate variations in the peptide binding modes. For example, the EF loop (residues 588–592) is significantly more impacted by the addition of canonical peptide JAK2-pep than by ErbB4-pep (Supplemental Table 3 and Figure 3). Residues within the EF loop are known to make several hydrophobic contacts to the +3 Leu of JAK2-pep (Supplemental Figure 1), which may explain the significant perturbations to these residues upon JAK2-pep addition.²¹ Similarly, several residues of the BG loop (E612, S613, and S617) produce chemical shifts uniquely upon the addition of JAK2-pep (BMRB ID:

27126), even though they were absent in the spectrum of free SH2B1 and upon the titration of the four other peptides. This suggests that the BG loop becomes more ordered upon JAK2-pep binding, which is consistent with the hydrophobic contacts apparent in the crystal structure between the +3 Leu of JAK2-pep and I609, P610 and L611 (Supplemental Figure 1B, PDB ID: 2HDX). The stabilization of the BG loop additionally aligns with the disfavorable entropy determined by ITC for the SH2B1/JAK2-pep interaction.

The three weak binding peptides (IR-pep, ANP32A-pep, and IGF1R-pep) also, not unexpectedly, appear to share a very similar binding interface as the tight binding peptides, as indicated by conserved chemical shift perturbations to residues in the β D sheet and BC loop (Supplemental Table 3 and Supplemental Figure 3). However, the titrations of these peptides did not significantly impact the chemical shifts of several residues that were important for tight peptide binding, including V589, I609, K575, and had a somewhat reduced impact on

TABLE 3 Phosphopeptide binding affinities to charge-swapped SH2B1 mutants reveal distinct roles of K575 and R578 in peptide binding^a

Peptide	SH2B1_Wildtype		SH2B1_K575E		SH2B1_R578E	
	Affinity class	K _d (μM)	K _d (μM)	Fold change from wildtype	K _d (μM)	Fold change from wildtype
JAK2-pep	Tight	0.320 ± 0.021*	118 ± 4	370	9.13 ± 0.90*	29
ErbB4-pep		0.542 ± 0.087*	93.5 ± 1.1	170	107 ± 3	200
IR-pep	Weak	30.3 ± 0.3	208 ± 21	6.9	580 ± 14	19
AN32A-pep		18.2 ± 0.1	124 ± 6	6.8	219 ± 15	12
IGF1R-pep		68.2 ± 2.6	450 ± 37	6.6	520 ± 4	7.6

^aThe tighter interactions were assessed by ITC (indicated by an asterisk*), while all other interactions were measured by NMR titration experiments. Values shown are averages from a minimum of triplicate measurements. Error values reported are the standard errors of the mean.

R578. The reduced chemical shift perturbations of these residues upon weak peptide binding compared to tight peptide binding suggests that contacts to these residues may be important for ligands to achieve high affinity binding to SH2B1. This finding supports our ITC data, which demonstrated that ErbB4-pep is part of a third class of peptide ligand distinct from JAK2-pep and the other three acidic residue-containing peptides. Taken together, NMR chemical shift mapping demonstrates that all five peptides bind SH2B1 using a similar binding interface, and we have identified several hydrophobic and charged residues that may play an additional role in promoting tight affinity binding by JAK2-pep and ErbB4-pep.

3.4 | SH2B1 mutagenesis studies reveal that residues K575 and R578 play significant and unique roles in binding to diverse peptides

Site-directed mutagenesis was employed to investigate specificity-determining SH2B1 residues and to further explore the origins of potential differences between peptide binding modes. We hypothesized that electrostatic interactions may govern the recognition of diverse peptides, considering that all five peptides studied here contain several acidic residues and are consequently predicted to be negatively charged at a physiological pH. In contrast, SH2B1 has a pI of 8.2, with a predicted approximate charge of +2 at a physiological pH, and has several exposed positively charged surfaces near the canonical ligand-binding interface.

To understand the role of key amino acids in the peptide binding modes, peptide binding affinity was measured using ITC and NMR to SH2B1 mutants containing alanine or charge-swapped point mutations at select positions. We have previously shown that a specific arginine in the C-terminal SH2 domain of phospholipase C-γ1 (PLCC_R716) forms a unique salt bridge to the +3 Asp of a non-cognate PLCC-binding peptide, which distinguishes the binding mode of this peptide from other ligands.³⁰ To determine whether this alternate binding mode is shared by SH2B1-binding peptides, the homologous residue to PLCC_R716 (SH2B1_R578) was analyzed to determine if it similarly discriminates for an acidic residue at position +3. Other positively charged residues near the known JAK2-pep binding interface, including K575 and R588, which exhibited chemical shift changes upon peptide

binding, were targeted since their proximity to the canonical JAK2-pep binding interface may allow them to differentially interact with diverse negatively charged peptides. Finally, we selected H591 due to its location in the key EF loop and the fact that this residue exhibited chemical shift changes upon binding all peptides. Taken together, the mutations tested were K575E, R578E, R588E, and H591A (Supplemental Figure 4).

The R588E and H591A mutations had minimal impact on peptide binding, with less than a three-fold change in peptide binding affinity. In contrast, the K575E and R578E mutations significantly reduced the binding affinity of all peptides, but by varying magnitudes (Table 3). The two tight binding peptides, JAK2-pep and ErbB4-pep, responded very similarly to both mutations. The SH2B1_K575E mutation had a pronounced impact on binding to these peptides, with affinities that were approximately 370- and 170-fold weaker (for JAK2-pep and ErbB4-pep, respectively) compared to wildtype SH2B1. Similarly, reduced affinities of approximately 30-fold and 200-fold were observed for binding of these two peptides to the charge-swapped mutant SH2B1_R578E. In contrast, the three weak binding peptides only experienced reduced affinities of approximately 7-fold in response to K575E mutagenesis and 10- to 20-fold in response to R578E mutagenesis, consistent with a less significant electrostatic effect. This is in qualitative agreement with the NMR chemical shift mapping data, which showed large chemical shift changes of K575 at upon the titration of JAK2-pep and ErbB4-pep as compared to no detectable change at this site for the three weak binding peptides. R578 shifts upon binding in all cases, although more dramatically for the tight binding peptides. These findings suggest that the K575 and R578 residues play significant roles in binding specifically to the tight affinity class of peptides, and that R578 may play an especially critical role in binding to ErbB4-pep.

4 | DISCUSSION

Several high-throughput array studies have determined that SH2B1 has specificity for peptides containing hydrophobic amino acids C-terminal to the pY of a peptide ligand, including a particularly strong preference for a leucine or isoleucine at the +3 position.^{19,20} Thus, it was surprising that additional studies using more targeted peptide

libraries (such as peptides derived from ErbB or insulin signaling proteins) found a preference of SH2B1 for peptides containing an acidic amino acid (Asp or Glu) at the +3 position.^{22,23} We have found that several peptides containing an acidic residue at +3 are indeed capable of binding SH2B1 well *in vitro*, although only one peptide, ErbB4-pep, binds SH2B1 with an affinity comparable to cognate ligand JAK2-pep (Table 2). This difference in affinities demonstrates that specificity is more nuanced than suggested simply by the nature of the amino acid at position +3.

Structural and biochemical data provide insights into how this dual binding specificity is achieved. A new high-resolution (1.4 Å) structure of the free SH2 domain of SH2B1 highlights the protein's inherently plastic structural features, which may allow it to adopt alternate conformations needed to bind different ligand classes. For example, the BG loop exhibits conformational movements up to 10 Å, in addition to more modest atomic movements of the DE and EF loops (Figure 2). Stabilization of the BG loop when bound to JAK2-pep may be a unique feature of JAK2-pep binding, which is consistent with the unfavorable entropy associated with this binding mode. The NMR chemical shift mapping data also indicate that interactions to residues of the EF loop (residues 588–592) are only present in the JAK2-pep binding mode, suggesting that the +3 acidic residue-containing peptides contact alternate surfaces on the SH2B1 interface.

In the absence of a hydrophobic residue at the +3 position, the presence of an acidic +3 residue is necessary, but not sufficient, to achieve high affinity binding. Our data, combined with a related structure, point to the features that likely enable ErbB4-pep, which contains a +3 Asp, to bind SH2B1 with high affinity. We found that the R578E mutation had a much more pronounced impact on ErbB4-pep binding (nearly 200-fold reduced affinity, compared to 7- to 30-fold for all other peptides). This behavior is reminiscent of another SH2 domain system, PLCC, in which the homologous residue (PLCC_R716) plays a unique and critical role in binding to a peptide containing a +3 Asp through novel salt bridge and hydrogen bond interactions that cause the peptide to bind in a different orientation across the interface.³⁰ Our data indicate that additional hydrophobic contacts to C-terminal peptide residues may be necessary for a peptide to bind with high affinity in the absence of a hydrophobic +3 residue. Numerous hydrophobic amino acids within the EF loop (including V589 and I609) are uniquely impacted by the tight-binding peptides (JAK2-pep and ErbB4-pep) and thus appear to discriminate between the tight and weak-binding peptides (IR-pep, AN32A-pep, and IGF1R-pep) (Figure 3 and Supplemental Table 3 and Figure 3). This loop contacts the +3 Leu of JAK2-pep,²¹ whereas upon binding to ErbB4-pep may undergo a conformational change, widening the groove allowing these sites to instead participate in favorable hydrophobic interactions to alternate peptide positions, such as +4 Pro or +5 Leu. Consistent with this idea, all three of the weak binding peptides exclusively contain charged and/or polar +4 and +5 amino acids that would be unable to form this type of hydrophobic interaction.

The diversity observed in the peptide binding modes of SH2B1 may be shared by additional SH2 domains, which would expand our understanding of the role of SH2 domains as key signaling hub

molecules. In addition to SH2B1 and PLCC, the βD6 residue has a basic side-chain in over half of the 120 known SH2 domains in humans (30 contain a lysine and 34 contain an arginine).⁴⁹ Similarly, the homologous residue to SH2B1_K575 (βD3), which is important for both JAK2-pep and ErbB4-pep binding, is conserved as a basic residue in approximately half of the human SH2 domains (59 of the 120 domains), and has been previously implicated in the discrimination of SH2 domain specificity classes.²⁶ 25 human SH2 domains contain a basic residue at both the βD3 and βD6 positions. A secondary binding mode driven by electrostatic interactions to the βD6 residue may, thus, be a broad mechanism of molecular recognition shared by numerous SH2 domain-containing proteins.

One approach to understand the prevalence of alternate ligand binding modes is to assess the diversity of structures observed in the SH2 domain family. When numerous structures of SH2 domain/peptide complexes solved to high resolution (< 3 Å) by X-ray crystallography are overlaid, it is apparent that the tertiary structures of SH2 domains are highly conserved, with RMSD values under 1 Å for nearly all molecular comparisons (after outlier rejection, Supplemental Figure 5 A). However, several of the protein loops, such as the BC, DE, EF, and BG loops, exhibit moderate conformational heterogeneity, which has been previously demonstrated to contribute to SH2 domain specificity.⁵⁰ This agrees well with the loop plasticity observed for SH2B1, and the distinct roles proposed for the EF and BG loops in binding to JAK2-pep. Several of the structures (e.g., peptide-bound SH2 domains of LCK, NCK1, PTPN11, and SRC) demonstrate hydrophobic contacts between residues of the EF loop and hydrophobic residues at the +3 position of the peptide. Likewise, hydrophobic or electrostatic interactions are also common between peptide residues and the BG loop (e.g., the peptide-bound SH2 domains of LCK, PIK3R1_C, PLCC/ErbB2-pep, and SRC). Thus, although the overall SH2 domain structure is well-conserved between homologues, conformational diversity of the EF and BG loops permit the formation of distinct bonding networks between these protein loops and the peptide ligand, and may thereby explain the differences in specificity classes observed between SH2 domains, and specifically between the peptide classes recognized by SH2B1.

Similarly, there is also plasticity apparent between the conformations of peptides when bound to SH2 domains, which further supports our findings that the hydrophobic and acidic classes of SH2B1-binding peptides likely rely on distinct bonding networks (Supplemental Figure 5B). While some SH2 domain specificity classes are known to adopt unique binding modes (such as the β-turn-induced bent conformation of GRB2-binding peptides⁵¹), peptides in the common extended conformation can also adopt a trajectory several angstroms higher or lower on the protein surface as compared to others. Similar to the conformational diversity of the EF and BG loops noted above, the differences observed between peptide conformations are largely driven by the formation of bonding networks to residues of the EF and BG loops, as well as to the central βD strand.

Understanding the diverse modes of peptide recognition utilized by SH2B1 will be instrumental to the identification of novel SH2B1-binding ligands with physiological implications in human signaling

pathways. For example, the ability of SH2B1 to bind ErbB4-pep with nanomolar affinity suggests a role for SH2B1 in ErbB signaling. ErbB receptor-mediated pathways regulate several cellular functions, including proliferation and migration, with consequent roles in cancer.^{52,53} As a result of its known role as an adaptor and enhancer in insulin, leptin, and growth hormone signaling pathways, SH2B1 has already been established as a key regulator of energy homeostasis, including the management of body weight and glucose metabolism, and has emerged as a candidate for medical research targeting obesity and diabetes.^{2,6} Through the identification of novel classes of peptide ligands, including acidic residue-containing peptides such as ErbB4-pep, we have demonstrated that SH2B1 may be involved in previously unrecognized signaling pathways with clinical implications in the treatment of additional diseases, including cancer. Peptidomimetic inhibitors of numerous SH2 domains, including those of STAT3, Grb2, Grb7, and SRC, have been extensively studied, with several molecules resulting in tumor reduction in *in vivo* mouse models of human cancers.^{54,55} The SH2 domain of SH2B1 may offer a similar platform for the development of pharmaceuticals for the treatment of numerous medical disorders, including obesity, diabetes, and cancer. We have identified several specificity-determining structural features of SH2B1, such as K575, R578, and residues of the EF loop, which may provide insights into the rational design of therapeutics that target the SH2 domain/phosphopeptide interface of SH2B1 with high affinity and specificity.

In summary, we have identified a peptide, ErbB4-pep, that binds SH2B1 with nanomolar affinity, driven largely by electrostatic interactions to residues K575 and R578. These residues are highly conserved amongst human SH2 domains, suggesting that this secondary electrostatically driven binding mode may be a common mechanism for the molecular recognition of phosphopeptides. A better understanding of the mechanisms driving the recognition of peptides containing acidic residues at the +3 position may facilitate the identification of additional novel peptides that can bind to SH2B1, or other SH2 domains, with tight affinity and with potential physiological implications. As a key regulator of body weight and glucose metabolism, understanding the peptide recognition patterns of SH2B1 and its wide range of peptide targets can also assist in the design of high affinity therapeutics to selectively target one peptide binding mode over another.

ACCESSION NUMBERS

The coordinates and structure factors for the structure of free SH2B1_3Δ have been deposited in the Protein Data Bank under the accession code 5W3R. The backbone chemical shift assignments for free SH2B1 and SH2B1/JAK2-pep have been deposited in the Biological Magnetic Resonance Bank under accession codes 27119 and 27126.

SUPPLEMENTARY MATERIAL

A figure of the cognate peptide binding mode of SH2B1 to JAK2-pep; A figure of the crystal packing contacts to SH2B1_3Δ; A plot of

¹H-¹⁵N-HSQC NMR chemical shift changes upon addition of peptides to SH2B1; A figure of the locations of SH2B1 residues targeted for mutagenesis studies; Structural overlays of numerous SH2 domain/peptide interactions; A table containing X-ray data collection and refinement statistics; A table comparing the SH2B1/phosphopeptide binding affinities measured by ITC versus NMR; A table of ¹H-¹⁵N-HSQC NMR chemical shift perturbations upon addition of peptides to SH2B1.

ACKNOWLEDGMENTS

We thank Drs. David McKay, Robert Batey, and Annette Erbse for training and assistance with X-ray crystallography data collection and refinement, and Dr. Arthur Pardi for assistance with NMR experimental troubleshooting. We also thank Neil Lloyd and Leslie Glustrom for their helpful comments on the manuscript. This work was supported by the National Science Foundation (MCB1121842 to D.S.W. and CHE-1454925 to X.G. and Z.T.) and the University of Colorado Boulder (Start-up fund to Z.T.). The Berkeley Center for Structural Biology (BCSB) is supported in part by the National Institutes of Health, National Institute of General Medical Sciences, and the Howard Hughes Medical Institute. The Advanced Light Source is supported by the Director, Office of Science, Office of Basic Energy Sciences, of the U.S. Department of Energy under Contract No. DE-AC02-05CH11231.

CONFLICT OF INTEREST

The authors declare that they have no conflict of interest with the contents of this article.

ORCID

Deborah S. Wuttke  <http://orcid.org/0000-0002-8158-8795>

REFERENCES

- [1] Liu BA, Nash PD. Evolution of SH2 domains and phosphotyrosine signalling networks. *Philos Trans R Soc B*. 2012;367(1602):2556-2573.
- [2] Rui L. SH2B1 regulation of energy balance, body weight, and glucose metabolism. *World J Diabetes*. 2014;5(4):511-526.
- [3] Duan C, Li M, Rui L. SH2-B promotes insulin receptor substrate 1 (IRS1)- and IRS2-mediated activation of the phosphatidylinositol 3-kinase pathway in response to leptin. *J Biol Chem*. 2004;279(42):43684-43691.
- [4] Diakonova M, Gunter DR, Herrington J, Carter-Su C. SH2-B β is a Rac-binding protein that regulates cell motility. *J Biol Chem*. 2002;277(12):10669-10677.
- [5] Desbuquois B, Carré N, Burnol AF. Regulation of insulin and type 1 insulin-like growth factor signaling and action by the Grb10/14 and SH2B1/B2 adaptor proteins. *FEBS J*. 2013;280:794-816.
- [6] Ren D, Li M, Duan C, Rui L. Identification of SH2-B as a key regulator of leptin sensitivity, energy balance, and body weight in mice. *Cell Metab*. 2005;2(2):95-104.
- [7] Nelms K, O'Neill TJ, Li S, Hubbard SR, Gustafson TA, Paul WE. Alternative splicing, gene localization, and binding of SH2-B to the insulin receptor kinase domain. *Mamm Genome*. 1999;10(12):1160-1167.

[8] Riedel H, Wang J, Hansen H, Yousaf N. PSM, an insulin-dependent, pro-rich, PH, SH2 domain containing partner of the insulin receptor. *J Biochem*. 1997;122(6):1105–1113.

[9] Kotani K, Wilden P, Pillay TS. SH2-B β is an insulin-receptor adaptor protein and substrate that interacts with the activation loop of the insulin-receptor kinase. *J Biochem*. 1998;335(1):103–109.

[10] Wang J, Riedel H. Insulin-like growth factor-I receptor and insulin receptor association with a Src homology-2 domain-containing putative adapter. *J Biol Chem*. 1998;273(6):3136–3139.

[11] O'brien KB, O'shea JJ, Carter-Su C. SH2-B family members differentially regulate JAK family tyrosine kinases. *J Biol Chem*. 2002;277: 8673–8681.

[12] Rui L, Mathews LS, Hotta I, Gustafson TA, Carter-Su C. Identification of SH2-B β as a substrate of the tyrosine kinase JAK2 involved in growth hormone signaling. *Mol Cell Biol*. 1997;17(11): 6633–6644.

[13] O'brien KB, Argetsinger LS, Diakonova M, Carter-Su C. YXXL motifs in SH2-B β are phosphorylated by JAK2, JAK1, and platelet-derived growth factor receptor and are required for membrane ruffling. *J Biol Chem*. 2003;278:11970–11978.

[14] Kurzer JH, Saharinen P, Silvennoinen O, Carter-Su C. Binding of SH2-B family members within a potential negative regulatory region maintains JAK2 in an active state. *Mol Cell Biol*. 2006;26(17):6381–6394.

[15] Kurzer JH, Argetsinger LS, Zhou Y-J, Kouadio J-LK, O'shea JJ, Carter-Su C. Tyrosine 813 is a site of JAK2 autophosphorylation critical for activation of JAK2 by SH2-B beta. *Mol Cell Biol*. 2004;24(10): 4557–4570.

[16] Rui L, Gunter DR, Herrington J, Carter-Su C. Differential binding to and regulation of JAK2 by the SH2 domain and N-terminal region of SH2-B β . *Mol Cell Biol*. 2000;20(9):3168–3177.

[17] Nishi M, Werner ED, Oh B-C, et al. Kinase activation through dimerization by human SH2-B. *Mol Cell Biol*. 2005;25(7):2607–2621.

[18] Rui L, Carter-Su C. Identification of SH2-B β as a potent cytoplasmic activator of the tyrosine kinase janus kinase 2. *Proc Natl Acad Sci U S A*. 1999;96(13):7172–7177.

[19] Huang H, Li L, Wu C, et al. Defining the specificity space of the human SRC homology 2 domain. *Mol Cell Proteomics*. 2008;7(4): 768–784.

[20] Tinti M, Kiemer L, Costa S, et al. The SH2 domain interaction landscape. *Cell Rep*. 2013;3(4):1293–1305.

[21] Hu J, Hubbard SR. Structural basis for phosphotyrosine recognition by the Src homology-2 domains of the adapter proteins SH2-B and APS. *J Mol Biol*. 2006;361(1):69–79.

[22] Liu BA, Jablonowski K, Shah EE, Engelmann BW, Jones RB, Nash PD. SH2 domains recognize contextual peptide sequence information to determine selectivity. *Mol Cell Proteomics*. 2010;9(11):2391–2404.

[23] Liu B. A, Engelmann BW, Jablonowski K, Higginbotham K, Stergachis AB, Nash PD. SRC homology 2 domain binding sites in insulin, IGF-1 and FGF receptor mediated signaling networks reveal an extensive potential interactome. *Cell Commun Signal*. 2012;10(1):1–23.

[24] Hause RJ, Leung KK, Barking JL, et al. Comprehensive binary interaction mapping of SH2 domains via fluorescence polarization reveals novel functional diversification of ErbB receptors. *PLoS One*. 2012;7(9):1–16.

[25] Hajicek N, Charpentier TH, Rush JR, Harden KT, Sondek J. Auto-inhibition and phosphorylation-induced activation of PLC- γ isoforms. *Biochemistry*. 2013;52(28):4810–4819.

[26] Songyang Z, Shoelson S, Chaudhuri M, et al. SH2 domains recognize specific phosphopeptide sequences. *Cell*. 1993;72:767–776.

[27] Mallis RJ, Brazin KN, Fulton DB, Andreotti AH. Structural characterization of a proline-driven conformational switch within the Itk SH2 domain. *Nat Struct Biol*. 2002;9(12):900–905.

[28] Breheny PJ, Laederach A, Fulton DB, Andreotti AH. Ligand specificity modulated by prolyl imide bond *cis/trans* isomerization in the Itk SH2 domain: A quantitative NMR study. *J Am Chem Soc*. 2003;125(51):15706–15707.

[29] Pascal SM, Singer A. U, Gish G, et al. Nuclear magnetic resonance structure of an SH2 domain of phospholipase C-gamma 1 complexed with a high affinity binding peptide. *Cell*. 1994;77(3):461–472.

[30] McKercher MA, Guan X, Tan Z, Wuttke DS. Multimodal recognition of diverse peptides by the C-terminal SH2 domain of phospholipase C- γ 1 protein. *Biochemistry*. 2017;56(16):2225–2237.

[31] McKercher MA, Wuttke DS. (2017) NMR chemical shift mapping of SH2 peptide interactions. In: Machida K, Liu BA, eds. *SH2 Domains: Methods and Protocols*. (). New York, NY: Springer; 2017: 269–290.

[32] Gasteiger E, Hoogland C, Gattiker A, et al. Protein identification and analysis tools on the ExPASy server. *Proteomics Protoc Handb*. 2005;571–607.

[33] Anthis NJ, Clore GM. Sequence-specific determination of protein and peptide concentrations by absorbance at 205 nm. *Protein Sci*. 2013;22(6):851–858.

[34] Goldfarb AR, Saidel LJ, Mosovich E. The ultraviolet absorption spectra of proteins. *J Biol Chem*. 1951;193(1):397–404.

[35] McKercher MA, Wuttke DS. (2017) Calorimetric measurement of SH2 domain ligand affinities. In: Machida K, Liu BA, eds. *SH2 Domains: Methods and Protocols*. New York, NY: Springer; 2017: 291–305.

[36] Battye TGG, Kontogiannis L, Johnson O, Powell HR, Leslie AGW. iMOSFLM: a new graphical interface for diffraction-image processing with MOSFLM. *Acta Crystallogr Sect D Biol Crystallogr*. 2011;67(Pt 4):271–281.

[37] Evans P. Scaling and assessment of data quality. *Acta Crystallogr Sect D Biol Crystallogr*. 2006;62(Pt 1):72–82.

[38] Winn MD, Ballard CC, Cowtan KD, et al. Overview of the CCP4 suite and current developments. *Acta Crystallogr Sect D Biol Crystallogr*. 2011;67(Pt 4):235–242.

[39] McCoy AJ, Grosse-Kunstleve RW, Adams PD, Winn MD, Storoni LC, Read RJ. Phaser crystallographic software. *J Appl Crystallogr*. 2007;40(Pt 4):658–674.

[40] Emsley P, Lohkamp B, Scott WG, Cowtan K. Features and development of Coot. *Acta Crystallogr Sect D Biol Crystallogr*. 2010;66(Pt 4): 486–501.

[41] Adams PD, Afonine PV, Bunkóczki G, et al. PHENIX: a comprehensive Python-based system for macromolecular structure solution. *Acta Crystallogr Sect D Biol. Crystallogr*. 2010;66(2):213–221.

[42] Chen VB, Arendall WB, Headd JJ, et al. MolProbity: all-atom structure validation for macromolecular crystallography. *Acta Crystallogr Sect D Biol Crystallogr*. 2010;66(1):12–21.

[43] Delaglio F, Grzesiek S, Vuister GW, Zhu G, Pfeifer J, Bax A. NMRPipe: a multidimensional spectral processing system based on UNIX pipes. *J Biomol NMR*. 1995;6(3):277–293.

[44] Vranken WF, Boucher W, Stevens TJ, et al. The CCPN data model for NMR spectroscopy: development of a software pipeline. *Proteins Struct Funct Genet*. 2005;59(4):687–696.

[45] Kemmer G, Keller S. Nonlinear least-squares data fitting in Excel spreadsheets. *Nat Protoc*. 2010;5(2):267–281.

[46] Farmer II, BT, Constantine KL, Goldfarb V, et al. Localizing the NADP⁺ binding site on the MurB enzyme by NMR. *Nature*. 1996;3(12):995–997.

[47] *The PyMOL Molecular Graphics System, Version 1.5.0.4*. Portland, OR: Schrodinger, LLC, 2010.

[48] Ladbury JE, Lemmon M. A, Zhou M, Green J, Botfield MC, Schlesinger J. Measurement of the binding of tyrosyl phosphopeptides to SH2 domains: a reappraisal. *Proc Natl Acad Sci USA*. 1995;92(8): 3199–3203.

[49] Liu B. SH2 domain alignment, 2010. <https://sites.google.com/site/sh2domain/alignment>. Accessed April 15, 2015.

[50] Kaneko T, Huang H, Zhao B, et al. Loops govern SH2 domain specificity by controlling access to binding pockets. *Sci Signal*. 2010;3:1–17.

[51] Rahuel J, Gay B, Erdmann D, et al. Structural basis for specificity of GRB2-SH2 revealed by a novel ligand binding mode. *Nat Struct Biol*. 1996;3:586–589.

[52] Hynes NE, Lane HA, Miescher F. ErbB receptors and cancer: the complexity of targeted inhibitors. *Nat Rev Cancer*. 2005;5(5):341–354.

[53] Hynes NE, Macdonald G. ErbB receptors and signaling pathways in cancer. *Curr Opin Cell Biol*. 2009;21(2):177–184.

[54] Fromer M, Shifman JM, Mirny LA. Tradeoff between stability and multispecificity in the design of promiscuous proteins. *PLoS Comput Biol*. 2009;5(12):e1000627

[55] Machida K, Mayer BJ. The SH2 domain: versatile signaling module and pharmaceutical target. *Biochim Biophys Acta*. 2005;1747(1):1–25.

[56] Eck MJ, Shoelson SE, Harrison SC. Recognition of a high-affinity phosphotyrosyl peptide by the Src homology-2 domain of p56. *Nature*. 1993;362(6415):87–91.

SUPPORTING INFORMATION

Additional Supporting Information may be found online in the supporting information tab for this article.

How to cite this article: McKercher MA, Guan X, Tan Z, Wuttke DS. Diversity in peptide recognition by the SH2 domain of SH2B1. *Proteins*. 2018;86:164–176. <https://doi.org/10.1002/prot.25420>